RSC Advances

PAPER

Cite this: *RSC Adv.*, 2016, **6**, 29210

Cu^{II} immobilized on guanidinated epibromohydrin functionalized γ-Fe_2O_3@TiO_2 (γ-Fe_2O_3@TiO_2-EG-Cu^{II}): a novel magnetically recyclable heterogeneous nanocatalyst for the green one-pot synthesis of 1,4-disubstituted 1,2,3-triazoles through alkyne–azide cycloaddition in water†

Roya Jahanshahi and Batool Akhlaghinia*

Received 1st March 2016
Accepted 14th March 2016

DOI: 10.1039/c6ra05468d

www.rsc.org/advances

Cu^{II} immobilized on guanidinated epibromohydrin functionalized γ-Fe_2O_3@TiO_2 (γ-Fe_2O_3@TiO_2-EG-Cu^{II}) as a novel magnetically recyclable heterogeneous catalyst was synthesized and characterized by various techniques such as FT-IR, TGA/DTA, HRTEM, XRD, EDX, VSM, ICP and elemental analysis. The catalyst demonstrated a superior catalytic activity towards the green one-pot synthesis of 1,4-disubstituted 1,2,3-triazoles *via* the three-component reaction between terminal alkynes, organic bromides, and sodium azide, in water. This method avoids isolation and handling of organic azides, because of their *in situ* generation. Importantly, the synthesized catalyst was separated easily by using an external magnet and recycled for six runs without appreciable leaching of copper from the surface of the catalyst.

1. Introduction

N-Heterocyclic compounds such as 1,2,3-triazoles, have tremendous applications in various research fields. In this context, numerous examples were reported in the literature including anti-HIV activity,[1,2] antibacterial activity,[3] antiallergic activity,[4] and selective β_3 adrenergic receptor agonism.[5] 1,2,3-Triazoles have also a range of important applications in biological science,[6] synthetic organic chemistry,[7] medicinal chemistry,[8] material chemistry[9] and industries such as dyes, corrosion inhibition, photostabilizers, photographic materials, and agrochemicals.[10] Thermal 1,3-dipolar cycloaddition of organic azides with alkynes was reported as the classical method for 1,2,3-triazoles preparation which suffered from some disadvantages such as elevated temperature, low yields of the products and lack of selectivity.[11] To remove these limitations, the most versatile protocol for the synthesis of 1,4-disubstituted 1,2,3-triazoles with high regioselectivity, low temperature reaction and enlarged scope has been developed, through the Cu(I)-catalyzed azide–alkyne cycloaddition (CuAAC, better known as click chemistry).[11–13] Because of thermodynamical instability of Cu(I) salts and also formation of undesired alkyne–alkyne coupling by-product, this method (CuAAC reaction) which has been extensively studied and widely used, was modified by *in situ* generation of Cu(I) species through the reduction of Cu(II) salts,[11,12,13b,14] oxidation of Cu(0) metal,[10c–i] and copper(II)/copper(0) comproportionation[15] or using Cu(I) salts in the presence of bases and/or ligands which protect Cu(I) intermediates from oxidation and disproportionation and hamper undesired side-product formation.[16]

Recently, heterogeneous catalysts have gained prominent attention in economical and environmentally benign chemical processes, due to their efficient recyclability and facile separation of the products. Numerous supports such as polymers,[17] aluminum oxyhydroxide nanofibers,[18] activated charcoal,[19] zeolites,[20] magnetic material,[21] alumina,[22] clay,[23] silica-supported N-heterocyclic carbene[24] and titanium dioxide,[25] have been attempted for CuAAC reaction. Moreover, solid supported Cu^{II} species as heterogeneous catalytic systems without reducing agents have been reported in alkyne–azide cycloaddition reaction.[26]

In recent years, magnetic nanoparticles (MNPs) have received remarkable attention by organic chemists as a new alternative to porous materials for homogeneous catalysts supporting.[27] Because of the magnetic nature of MNPs, the appropriate removal and recycling of the MNPs-supported catalysts is feasible by means of an external magnet. This separation approach is not time-consuming in comparison with standard methods (filtration and centrifugation), and prevents the heterogeneous catalyst loss during the separation process. Additionally, it increases the purity of the products, as well as

Department of Chemistry, Faculty of Sciences, Ferdowsi University of Mashhad, Mashhad 9177948974, Iran. E-mail: akhlaghinia@um.ac.ir; Fax: +98-51-3879-5457; Tel: +98-51-3880-5527

† Electronic supplementary information (ESI) available: General information, spectral data of organic compounds. See DOI: 10.1039/c6ra05468d

optimizing the operational costs.[28] Besides, a great deal of efforts have been devoted to the incorporation of MNPs into core shell structures, in order to control the size, shape and magnetic features of the hybrid materials.[29] Coating of the MNPs avoids their aggregation/oxidation and serves as the catalyst platform.[30]

On the other hand, it is worth mentioning that a recyclable catalyst needs an appropriate reaction media for implementation in large scale in chemical industries. Recently, organic reactions in water as a benign reaction media, have attracted a number of interest in both academic and industrial research, because water is nontoxic, readily available, environmentally friendly and cheap. Furthermore, reactions in aqueous media represent unique selectivities and reactivities, as well as cleaner chemical processes, in comparison with those performed in organic media.

As part of our continuing interests in developing new heterogeneous catalysts,[31] in the synthetic organic chemistry, herein, we wish to report the preparation of Cu^{II} immobilized on guanidinated epibromohydrin functionalized γ-Fe_2O_3@TiO_2 (γ-Fe_2O_3@TiO_2-EG-Cu^{II}) as a novel and magnetically recyclable heterogeneous catalyst (Scheme 1). The catalytic activity of γ-Fe_2O_3@TiO_2-EG-Cu^{II}, was proved for the one-pot synthesis of 1,4-disubstituted 1,2,3-triazoles, through alkyne–azide cycloaddition, in water (see Scheme 2).

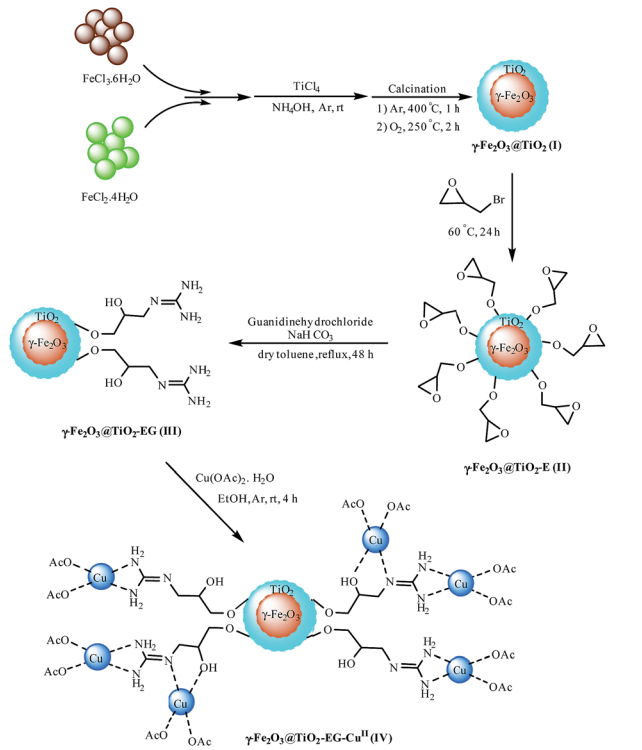

Scheme 1 Preparation of Cu^{II} immobilized on guanidinated epibromohydrin functionalized γ-Fe_2O_3@TiO_2 (γ-Fe_2O_3@TiO_2-EG-Cu^{II}).

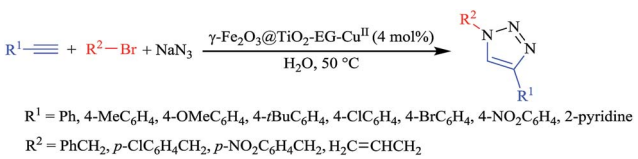

Scheme 2 Synthesis of different structurally 1,4-disubstituted 1,2,3-triazoles in the presence of γ-Fe_2O_3@TiO_2-EG-Cu^{II}, in water.

2. Experimental

2.1. Materials

All chemical reagents and solvents were purchased from Merck and Sigma-Aldrich chemical companies and were used as received without further purification. γ-Fe_2O_3/TiO_2 nanoparticles were prepared by the previously reported method in literature.[32]

2.2. Instrumentation analysis

The purity determinations of the products and the progress of the reactions were accomplished by TLC on silica gel polygram STL G/UV 254 plates. The melting points of the products were determined with an Electrothermal Type 9100 melting point apparatus. The FTIR spectra were recorded on pressed KBr pellets using an AVATAR 370 FT-IR spectrometer (Therma Nicolet spectrometer, USA) at room temperature in the range between 4000 and 400 cm^{-1} with a resolution of 4 cm^{-1}, and each spectrum was the average of 32 scans. NMR spectra were recorded on a NMR Bruker Avance spectrometer at 400 and 300 MHz in $CDCl_3$ as solvent in the presence of tetramethylsilane as the internal standard and the coupling constants (J values) are given in Hz. Elemental analyses were performed using a Thermo Finnigan Flash EA 1112 Series instrument (furnace: 900 °C, oven: 65 °C, flow carrier: 140 mL min^{-1}, flow reference: 100 mL min^{-1}). Mass spectra were recorded with a CH7A Varianmat Bremem instrument at 70 eV electron impact ionization, in m/z (rel%). Thermogravimetric analyses (TGA and DTG) were carried out using a Shimadzu Thermogravimetric Analyzer (TG-50) in the temperature range of 25–900 °C at a heating rate of 10 °C min^{-1}, under air atmosphere. HRTEM analysis was performed using HRTEM microscope (Philips CM30). Inductively coupled plasma (ICP) was carried out on a Varian, VISTA-PRO, CCD, Australia. Elemental compositions were determined with an SC7620 energy-dispersive X-ray analysis (EDX) presenting a 133 eV resolution at 20 kV. Room temperature magnetization isotherms were obtained using a vibrating sample magnetometer (VSM, LakeShore 7400). X-ray powder diffraction (XRD) was performed on a X'Pert Pro MPD diffractometer with Cu K_α ($\lambda = 0.154$ nm) radiation. All yields refer to isolated products after purification by recrystallization.

2.3. Preparation of γ-Fe_2O_3@TiO_2 nanoparticles (I)

$FeCl_3 \cdot 6H_2O$ (5.11 g, 18.9 mmol) and $FeCl_2 \cdot 4H_2O$ (2.21 g, 17.43 mmol) were dissolved in deionized water (50 mL) under argon atmosphere at room temperature. The solution was stirred magnetically for 5 min, and then titanium tetrachloride (2 mL, 18 mmol) was added into the solution. NH_4OH solution (0.6 M, 400 mL) was then added drop by drop (drop rate = 1 mL min^{-1}) into the solution using a syringe pump under vigorous stirring at room temperature. When pH was adjusted to 9.0, addition of

NH_4OH solution was stopped. The mixture was diluted with 200 mL deionized water and stirred vigorously for 30 min at 50 °C, in water bath. Then the mixture was placed on a strong magnet and the particles were then separated from the solution. The particles were washed with deionized water (5 × 20 mL) and then dried at 40 °C for 24 h. Afterwards, the particles were crushed and calcinated under argon atmosphere at 400 °C for 1 h to obtain crystallized anatase TiO_2. Then the obtained nanoparticles were calcinated under oxygen at 250 °C for 2 h. γ-Fe_2O_3@TiO_2 (**I**) was stored in a desiccator for further use.

2.4. Preparation of epibromohydrin functionalized γ-Fe_2O_3@TiO_2 (γ-Fe_2O_3@TiO_2-E) (II)

γ-Fe_2O_3@TiO_2 nanoparticles (**I**) (2 g) was dispersed in 6 mL pure epibromohydrin by sonication for 30 min. The resultant suspension was heated at 60 °C with vigorous stirring. After 24 h, epibromohydrin-functionalized γ-Fe_2O_3@TiO_2-E (**II**) was separated by an external magnet and washed with MeOH (5 × 10 mL) until removing additional amount of epibromohydrin and then dried at 40 °C under vacuum for 14 h.

2.5. Preparation of guanidinated epibromohydrin functionalized γ-Fe_2O_3@TiO_2 (γ-Fe_2O_3@TiO_2-EG) (III)

The γ-Fe_2O_3@TiO_2-E (**II**) (1.5 g), was dispersed in dry toluene (7 mL), by placing in an ultrasonic bath for 20 min. Subsequently, guanidine hydrochloride (0.38 g, 0.004 mmol) and sodium bicarbonate (0.67 g, 0.008 mmol) were added and the mixture was refluxed for 48 h. Then, the final product was separated by magnetic decantation and washed with dry CH_2Cl_2 (3 × 15 mL) and EtOH (3 × 15 mL), respectively and then dried under vacuum at 40 °C.

2.6. Preparation of Cu^{II} immobilized on guanidinated epibromohydrin functionalized γ-Fe_2O_3@TiO_2 (γ-Fe_2O_3@TiO_2-EG-Cu^{II}) (IV)

To a solution of $Cu(OAc)_2 \cdot H_2O$ (0.6 mmol, 0.11 g) in absolute EtOH (5 mL), γ-Fe_2O_3@TiO_2-EG (**III**) (1 g) was added at room temperature. The reaction mixture was stirred under argon atmosphere for 4 h. The resulting suspension was separated and washed with acetone (4 × 5 mL) and ethanol (4 × 5 mL), respectively and then dried under vacuum at ambient temperature for 16 h.

2.7. Typical procedure for preparation of 1-benzyl-4-phenyl-1*H*-1,2,3-triazole (4a)

γ-Fe_2O_3@TiO_2-EG-Cu^{II} (0.054 g, 4 mol%), was added to a solution of phenylacetylene (0.102 g, 1 mmol), benzyl bromide (0.171 g, 1 mmol) and NaN_3 (0.078 g, 1.2 mmol) in H_2O (5 mL). The mixture was magnetically stirred at 50 °C, for 5 min and the progress of the reaction was monitored by TLC (*n*-hexane : EtOAc, 3 : 1). Upon the completion of the reaction, the catalyst was removed by an external magnet, washed with methanol (2 × 10 mL) and dried overnight to be ready for the next run. The resulting mixture was diluted with deionized water (10 mL) and extracted with EtOAc (3 × 15 mL). The organic layer was dried over anhydrous Na_2SO_4, followed by evaporation under reduced pressure to remove the solvent. The residue was purified by recrystallization from ethanol to afford 1-benzyl-4-phenyl-1*H*-1,2,3-triazole (0.22 g, 94%).

3. Results and discussion

3.1. Characterization of γ-Fe_2O_3@TiO_2-EG-Cu^{II} (IV)

According to the pathway shown in Scheme 1, γ-Fe_2O_3@TiO_2-EG-Cu^{II} was synthesized as a novel efficient and reusable heterogeneous catalyst. This newly synthesized catalyst was fully characterized by different techniques such as Fourier transform infrared spectroscopy (FT-IR), thermogravimetric analysis/differential thermal analysis (TGA/DTA), high resolution transmission electron microscopy (HRTEM), X-ray powder diffraction (XRD), energy-dispersive X-ray analysis (EDX), vibrating sample magnetometer (VSM), inductively coupled plasma (ICP) and elemental analysis (CHN). The results obtained from these techniques, confirmed the successful preparation of the new catalyst.

Fig. 1 illustrates the FT-IR spectra of γ-Fe_2O_3@TiO_2 (**I**), epibromohydrin functionalized γ-Fe_2O_3@TiO_2 (**II**), guanidinated epibromohydrin functionalized γ-Fe_2O_3@TiO_2 (**III**) and Cu^{II} immobilized on guanidinated epibromohydrin functionalized γ-Fe_2O_3@TiO_2 (γ-Fe_2O_3@TiO_2-EG-Cu^{II} (**IV**)). As can be seen, the stretching vibration of Fe–O bond in γ-Fe_2O_3 was assigned at around 698–571 cm^{-1},[33] which was covered by the broad characteristic stretching vibration band of Ti–O at 850–500 cm^{-1} in the TiO_2 lattice.[34] Furthermore, the absorption band at 1619 cm^{-1} (related to bending vibration) and the broad band appearing at 3500–3100 cm^{-1} (related to stretching vibration of both symmetrical and asymmetrical modes) were attributed to the physisorbed water and the hydroxyl groups which are attached to the surface of γ-Fe_2O_3@TiO_2.[35] The epoxy ring which was grafted to the γ-Fe_2O_3@TiO_2 framework was recognized by the methylene C–H stretching and bending vibration bands at 2923–2872 and 1454 cm^{-1}, respectively.[36] An absorption band at 1112 cm^{-1} was attributed to C–O–C vibrational stretching. These results indicated that the γ-Fe_2O_3@TiO_2 surface has been immobilized by covalent bonded organic epoxy rings. Ring opening of epoxy ring with guanidine was asserted by appearance of the absorption bands around 3378 and 1454 cm^{-1} corresponding to the N–H and C–N stretching vibrations, respectively.[35c] Absorption bands at 428, and 450 cm^{-1} document the coordination of Cu^{II} on guanidinated epibromohydrin functionalized γ-Fe_2O_3@TiO_2 which is allocated to Cu–N and Cu–O vibrations, respectively.[31a] These two absorption bands were covered by stretching vibration frequencies of Fe–O and Ti–O bonds. Upon coordination of Cu^{II}, the intensities of $-NH_2$ and probably –OH stretching frequencies (at around 3378–3162 cm^{-1}) were diminished, significantly. The –NH bending vibration (positioned at 1617 cm^{-1}) and probably OH bending vibration (positioned at 1619 cm^{-1}) were also shifted to lower frequencies due to coordination with Cu^{II}. Moreover C–N stretching vibration (positioned at 1454 cm^{-1}) and C=N stretching vibration (positioned at 1662 cm^{-1}), were shifted to lower frequencies assigned to coordination with Cu^{II}. Also, peaks depicted at 1634 and 1401 cm^{-1} in the spectrum of γ-

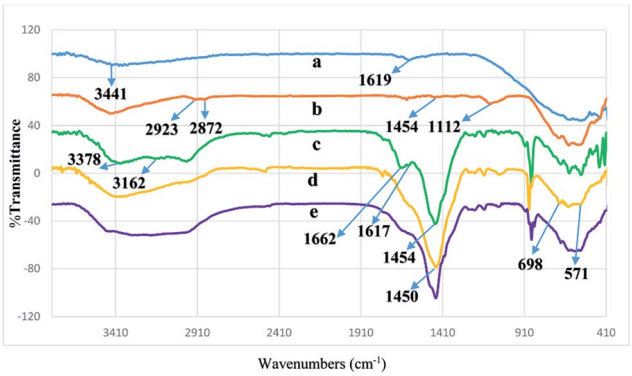

Fig. 1 FT-IR spectrum of (a) γ-Fe_2O_3@TiO_2 nanoparticles (I); (b) epibromohydrin functionalized γ-Fe_2O_3@TiO_2 (II); (c) guanidinated epibromohydrin functionalized γ-Fe_2O_3@TiO_2 (III); (d) Cu^{II} immobilized on guanidinated epibromohydrin functionalized γ-Fe_2O_3@TiO_2 (γ-Fe_2O_3@TiO_2-EG-Cu^{II} (IV)); (e) 6th recovered γ-Fe_2O_3@TiO_2-EG-Cu^{II}.

Fe_2O_3@TiO_2-EG-Cu^{II} were related to COO (in acetate),[33] confirming the presence of Cu in the catalyst. These absorption bands were covered by broad and strong C–N stretching vibration frequency.

The thermogravimetric analysis/differential thermal analysis (TGA/DTA) of γ-Fe_2O_3@TiO_2-EG-Cu^{II} was used to determine the thermal stability and content of organic functional groups on the surface of the MNPs (Fig. 2). TGA curve of γ-Fe_2O_3@TiO_2-EG-Cu^{II} showed the weight loss below 200 °C, which was related to the adsorbed water molecules on the support. The organic parts were decomposed completely in the temperature range of 200–670 °C (17.23 wt%). According to the TGA, the amount of organic segment supported on γ-Fe_2O_3@TiO_2 is estimated to be 0.70 mmol g^{-1}. These results were in a good agreement with the elemental analysis data (N = 3.01% and C = 7.02%) and ICP. The ICP analysis showed that 0.74 mmol of copper was anchored on 1.000 g of the catalyst.

HRTEM images of γ-Fe_2O_3@TiO_2-EG-Cu^{II} displayed a dark γ-Fe_2O_3 core with the average size of about 10–20 nm which was surrounded by a grey titania shell with a thickness of about 5–10 nm (Fig. 3).

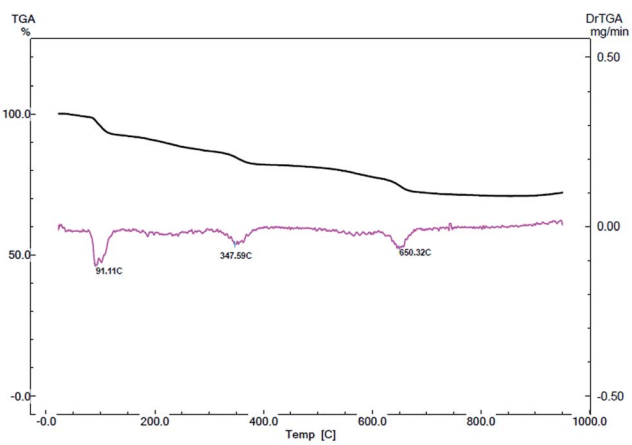

Fig. 2 Thermogram of γ-Fe_2O_3@TiO_2-EG-Cu^{II}.

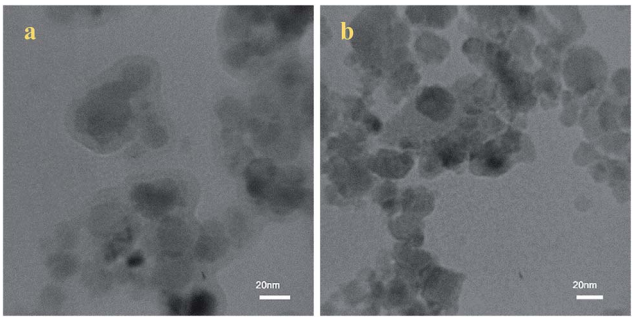

Fig. 3 HRTEM images of γ-Fe_2O_3@TiO_2-EG-Cu^{II} (a and b).

XRD measurement was used to identify the crystalline structure of γ-Fe_2O_3@TiO_2 MNPs. As shown in Fig. 4, all the peaks which can be indexed to (2 2 0), (3 1 1), (4 0 0), (4 2 2), (5 1 1) and (4 4 0) reflections, agree well with the cubic structure of maghemite (γ-Fe_2O_3) (JCPDS file no. 04-0755). In addition, weak diffraction peaks appeared at angles corresponding to (0 1 1), (0 0 4) and (0 2 0) crystallographic faces, could be assigned to anatase XRD diffraction peaks. The average crystallite size of maghemite and TiO_2 (anatase), calculated using the Debye–Scherrer equation $d = K\lambda/(\beta \cos \theta)$ are about 13 and 7 nm, respectively.

The energy-dispersive X-ray analysis (EDX) reveals the existence of C, O, Fe, Ti and Cu elements (Fig. 5). This analysis confirms that Cu^{II} is supported on guanidinated epibromohydrin functionalized γ-Fe_2O_3@TiO_2 (γ-Fe_2O_3@TiO_2-EG).

The magnetization curves of γ-Fe_2O_3@TiO_2 and γ-Fe_2O_3@TiO_2-EG-Cu^{II} were measured at ambient temperature with a vibrating sample magnetometry (VSM). As illustrated in Fig. 6, the value of saturation magnetic moments of γ-Fe_2O_3@TiO_2 NPs (Fig. 6a) and γ-Fe_2O_3@TiO_2-EG-Cu^{II} (Fig. 6b) are 23.79 and 22.12 emu g^{-1}, respectively. It indicates both γ-Fe_2O_3@TiO_2 and γ-Fe_2O_3@TiO_2-EG-Cu^{II} are superparamagnetic. Small decreasing in the saturation magnetization of γ-Fe_2O_3@TiO_2 NPs after the surface grafting, can be attributed to the contribution of the non-magnetic materials.

3.2. Catalytic synthesis of 1,4-disubstituted 1,2,3-triazoles

After the successful preparation and full characterization of the γ-Fe_2O_3@TiO_2-EG-Cu^{II}, its catalytic activity was examined for

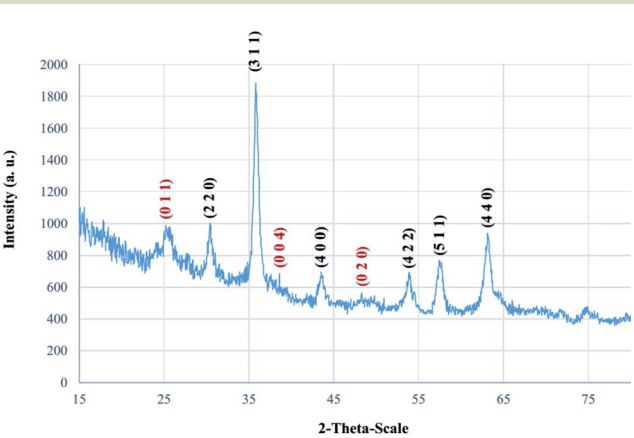

Fig. 4 XRD pattern of γ-Fe_2O_3@TiO_2 MNPs.

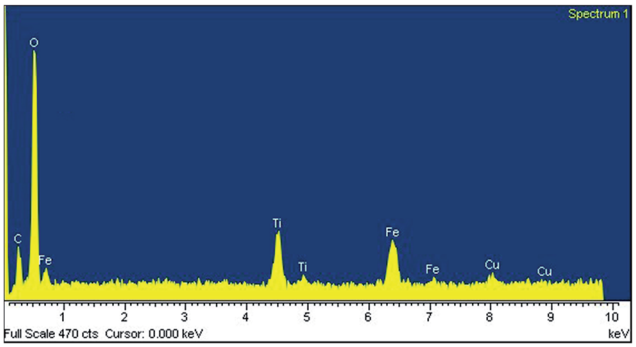

Fig. 5 EDX analysis of γ-Fe_2O_3@TiO_2-EG-Cu^{II}.

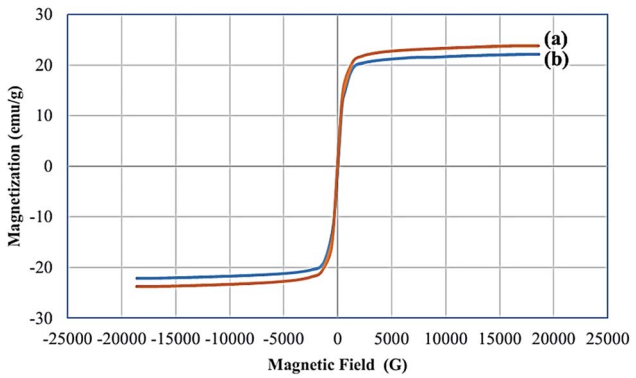

Fig. 6 Magnetization curves of (a) γ-Fe_2O_3@TiO_2 nanoparticles (I) and (b) γ-Fe_2O_3@TiO_2-EG-Cu^{II}.

the green one-pot synthesis of 1,4-disubstituted 1,2,3-triazoles from the reaction of various terminal alkynes, different organic bromides, and sodium azide (1,3-dipolar Huisgen cycloaddition reaction), in water (Scheme 2).

To find an appropriate reaction medium for the preparation of 1,4-disubstituted 1,2,3-triazoles in the presence of the catalytic amount of γ-Fe_2O_3@TiO_2-EG-Cu^{II}, the one pot reaction between phenylacetylene (1 mmol), benzyl bromide (1 mmol), and sodium azide (1.2 mmol), was selected as a model reaction. The model reaction behaviour was studied under a variety of conditions, and the results are summarized in Table 1. It can be seen that, when the model reaction was carried out at 100 °C in aqueous media, in the absence of the catalyst, no desired product was formed, even after a prolonged reaction time (Table 1, entry 1). Similarly, in the presence of (**I**), (**II**) and (**III**) as catalyst, the product yields were poor, even after 3 h (Table 1, entries 2–4). This reaction gives high yields of 1-benzyl-4-phenyl-1*H*-1,2,3-triazole (**4a**), in the presence of γ-Fe_2O_3@TiO_2-EG-Cu^{II} (Table 1, entry 5). Then, we investigated the effect of different temperatures on the model reaction (Table 1, entries 6–8). According to the data of Table 1, the best result was obtained at 50 °C (Table 1, entry 6). The model reaction was performed in the presence of different amounts of the catalyst (Table 1, entries 9–11).

Increasing the amount of the catalyst to 5 mol% showed no further increase in the yield of the product. However, decreasing the catalyst loading, led to lower product yield, in longer reaction time.

During our optimization studies, screening solvent free conditions and different solvents (Table 1, entries 12–16), revealed that H_2O clearly stands out as the solvent of choice

Table 1 One-pot synthesis of 1-benzyl-4-phenyl-1*H*-1,2,3-triazole under different reaction conditions

Entry	Molar ratio **1 : 2 : 3**	Catalyst (mol%)	Temp. (°C)	Solvent	Time (min)	Isolated yield (%)
1	1 : 1 : 1.2	None	100	H_2O	15 h	—
2[a]	1 : 1 : 1.2	0.054 g	100	H_2O	3 h	Trace
3[b]	1 : 1 : 1.2	0.054 g	100	H_2O	3 h	Trace
4[c]	1 : 1 : 1.2	0.054 g	100	H_2O	3 h	Trace
5	1 : 1 : 1.2	4	100	H_2O	5	94
6	**1 : 1 : 1.2**	**4**	**50**	**H_2O**	**5**	**94**
7	1 : 1 : 1.2	4	40	H_2O	1 h	62
8	1 : 1 : 1.2	4	r.t.	H_2O	1 h	41
9	1 : 1 : 1.2	3	50	H_2O	30	89
10	1 : 1 : 1.2	2	50	H_2O	30	74
11	1 : 1 : 1.2	5	50	H_2O	5	94
12	1 : 1 : 1.2	4	50	—	45	49
13	1 : 1 : 1.2	4	50	MeOH	30	57
14	1 : 1 : 1.2	4	50	MeOH : H_2O (1 : 1)	30	83
15	1 : 1 : 1.2	4	50	CH_3CN	30	Trace
16	1 : 1 : 1.2	4	50	THF	30	Trace
17	1 : 1 : 1	4	50	H_2O	10	65
18	1 : 1 : 1.1	4	50	H_2O	10	76
19	1 : 1 : 1.4	4	50	H_2O	5	94
20[d]	1 : 1 : 1.2	4	50	H_2O	15	90

[a] The reaction was performed in the presence of γ-Fe_2O_3@TiO_2 (**I**). [b] The reaction was performed in the presence of γ-Fe_2O_3@TiO_2-E (**II**). [c] The reaction was performed in the presence of γ-Fe_2O_3@TiO_2-EG (**III**). [d] The reaction was performed by using benzyl chloride instead of benzyl bromide.

with its fast reaction rate, high isolated yield and selectivity. It can be seen that, applying lower amounts of sodium azide resulted in 65% and 76% yields of the product, in water after a long time (Table 1, entries 17–18).

However, higher amounts of sodium azide had no more effect on the reaction progress (Table 1, entry 19). The obtained results demonstrated that the γ-Fe_2O_3@TiO_2-EG-Cu^{II} catalyst exhibits promising catalytic activity in water at 50 °C, with enhanced regioselectivity, towards the desired 1,4-disubstituted 1,2,3-triazole product (Table 1, entry 6). To probe the reaction scope and performance of γ-Fe_2O_3@TiO_2-EG-Cu^{II} catalyst, we also examined benzyl chloride (instead of benzyl bromide) under the optimized reaction conditions. Control experiment conducted in the presence of benzyl chloride illustrated the longer reaction time, due to the lower activity of benzyl chloride (Table 1, entry 20).

With the optimized reaction conditions in hand, we then investigated the generality and versatility of this method. The reaction was extended to various structurally diverse terminal alkynes and organic bromides (Table 2). In all cases, [3 + 2] cycloadditions were complete in a short time and 1,2,3-triazole derivatives were isolated in good to excellent yields. Using this methodology in the reaction of sodium azide, benzyl or allyl bromides with different terminal alkynes, produced only one of the possible regioisomers, as expected. The same methodology was successfully applied to the aryl acetylenes bearing both electron-releasing and electron-withdrawing groups attached to the aromatic ring. Additionally, the heteroaryl substituted acetylenes (2-ethynylpyridine) underwent clean reactions to produce the corresponding triazoles (Table 2, entries 8, 13 and 18). Excitingly, the results shown in Table 2 (entries 9–18) demonstrate that the reaction was compatible successfully with a broad range of substituted benzyl bromides. In an attempt to broaden the scope of our methodology, the possibility of performing the reaction with allyl bromide instead of benzyl bromide was also investigated. From Table 2, it can be observed that the Huisgen 1,3-dipolar cycloaddition reaction of terminal alkynes and allyl bromide proceeded smoothly and the corresponding 1,4-disubstituted 1,2,3-triazoles were obtained in high yields (Table 2, entries 19–22).

With this catalyst, a safe and efficient three-component reaction for the regioselective generation of 1,4-disubstituted 1,2,3-triazoles has been developed. The method avoids isolation and handling of potentially unstable organic azides and provides the triazole products in pure form. The scope of the cycloaddition using our catalyst is quite broad; various terminal alkynes react readily with benzyl and allyl bromides at 50 °C, in water.

However, having at least two active sites in each ligand that has been attached to the support (see Scheme 1), leads to high copper loading capacity of the catalyst, as this has been confirmed by inductively coupled plasma (ICP). Accordingly, γ-

Table 2 Huisgen 1,3-dipolar cycloaddition catalyzed by γ-Fe_2O_3@TiO_2-EG-Cu^{II}

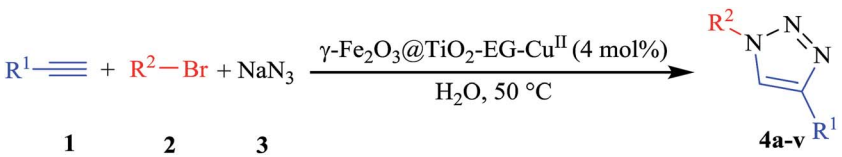

Entry	R^1	R^2	Product	Time (min)	Isolated yield (%)
1	Ph	$PhCH_2$	**4a**	5	94
2	4-MeC_6H_4	$PhCH_2$	**4b**	10	92
3	4-$MeOC_6H_4$	$PhCH_2$	**4c**	20	91
4	4-*t*-BuC_6H_4	$PhCH_2$	**4d**	35	88
5	4-ClC_6H_4	$PhCH_2$	**4e**	5	95
6	4-BrC_6H_4	$PhCH_2$	**4f**	6	94
7	4-$NO_2C_6H_4$	$PhCH_2$	**4g**	5	96
8	2-Pyridine	$PhCH_2$	**4h**	20	90
9	Ph	*p*-$ClC_6H_4CH_2$	**4i**	10	93
10	4-MeC_6H_4	*p*-$ClC_6H_4CH_2$	**4j**	20	92
11	4-$MeOC_6H_4$	*p*-$ClC_6H_4CH_2$	**4k**	30	90
12	4-*t*-BuC_6H_4	*p*-$ClC_6H_4CH_2$	**4l**	40	86
13	2-Pyridine	*p*-$ClC_6H_4CH_2$	**4m**	33	88
14	Ph	*p*-$NO_2C_6H_4CH_2$	**4n**	20	91
15	4-MeC_6H_4	*p*-$NO_2C_6H_4CH_2$	**4o**	35	89
16	4-$MeOC_6H_4$	*p*-$NO_2C_6H_4CH_2$	**4p**	35	86
17	4-*t*-BuC_6H_4	*p*-$NO_2C_6H_4CH_2$	**4q**	60	86
18	2-Pyridine	*p*-$NO_2C_6H_4CH_2$	**4r**	35	84
19	Ph	CH_2CHCH_2	**4s**	30	90
20	4-MeC_6H_4	CH_2CHCH_2	**4t**	42	87
21	4-$MeOC_6H_4$	CH_2CHCH_2	**4u**	50	84
22	4-*t*-BuC_6H_4	CH_2CHCH_2	**4v**	75	82

Table 3 Comparison of various catalysts in the synthesis of 1-benzyl-4-phenyl-1*H*-1,2,3-triazole

Entry	Catalyst	Reagents and reaction condition	Time (h)	Yield (%)	Ref.
1	Cu(II)-PBS-HPMO[a]	Phenylacetylene (1.1 mmol), benzyl bromide (1 mmol), NaN_3 (1.2 mmol), catalyst (10 mg), H_2O, 100 °C	3.5	96	26*a*
2	MNPs@BiimCu(II)[b]	Phenylacetylene (1 mmol), benzyl bromide (1 mmol), NaN_3 (1.1 mmol), catalyst (0.85 mol%), H_2O, r.t.	1	92	26*b*
3	Cu^{II}–hydrotalcite	Phenylacetylene (0.44 mmol), benzyl azide (0.37 mmol), catalyst (10 mg), ACN, r.t.	6	86	26*c*
4	Alumina-supported Cu(II)	Phenylacetylene (1 mmol), benzyl bromide (1 mmol), NaN_3 (1 mmol), catalyst (10 mol%), ball-milling/600 rpm	1	96	26*e*
5	Copper(II) acetate	Phenylacetylene (1.2 mmol), benzyl azide (1 mmol), catalyst (20 mol%), H_2O, r.t.	20	77	39
6	$CuCl_2/CuSO_4 \cdot 5H_2O$	Phenylacetylene (0.5 mmol), benzyl bromide (0.6 mmol), NaN_3 (0.6 mmol), catalyst (0.025 mmol), MeOH, r.t.	8	82/83	40
7	Ammonium salt-tagged NHC–Cu(I) complexes	Phenylacetylene (1.2 mmol), benzyl bromide (1.0 mmol), NaN_3 (1.2 mmol), catalyst (5 mol%), H_2O, r.t.	6	98	41
8	Copper nanoparticles on charcoal	Phenylacetylene (1 mmol), benzyl bromide (1 mmol), NaN_3 (1.1 mmol), catalyst (1 mol%), H_2O, 100 °C	0.6	91	42
9	CuNPs/MagSilica[c]	Phenylacetylene (1 mmol), benzyl bromide (1 mmol), NaN_3 (1.1 mmol), catalyst (40 mg), H_2O, 70 °C	1	98	30
10	Silica–Cu_2O	Phenylacetylene (1.2 mmol), benzyl chloride (1 mmol), NaN_3 (1 mmol), 0.2 g catalyst (5 mol% Cu), H_2O, r.t.	3.5	96	43
11	Silica-APTS-Cu(I)[d]	Phenylacetylene (0.5 mmol), benzyl bromide (0.5 mmol), NaN_3 (0.5 mmol), catalyst (5 mol%), EtOH, 78 °C	24	92	24
12	MNPs@FGly[e]	Phenylacetylene (0.5 mmol), benzyl bromide (0.5 mmol), NaN_3 (0.5 mmol), sodium ascorbate (10 mol%), Cu (0.5 mol%), H_2O/*t*-BuOH; (3/1), 55 °C	2	99	44
13	$CuSO_4 \cdot 5H_2O$	Phenylacetylene (1.5 equiv.), benzyl azide (1 equiv.), $N_2H_4 \cdot H_2O$ azide (1 equiv.), catalyst (0.1 equiv.), H_2O, r.t.	45 min	95	14*h*
14	γ-Fe_2O_3@TiO_2-EG-Cu^{II}	Phenylacetylene (1 mmol), benzyl bromide (1 mmol), NaN_3 (1.2 mmol), catalyst (4 mol%), H_2O, 50 °C	5 min	94	Present study

[a] Cu(II)-porphyrin-bridged silsesquioxane bridged hybrid periodic mesoporous organosilica. [b] Biimidazole Cu(II) ion complexes immobilized on core–shell magnetic nanoparticles. [c] Copper nanoparticles on silica coated maghemite nanoparticles. [d] Copper(I) on 3-aminopropyl functionalized silica. [e] Fe_3O_4–silica-coated@functionalized 3-glycidoxypropyltrimethoxysilane.

Fe_2O_3@TiO_2-EG-Cu^{II} catalyst was exhibited much more catalytic efficiency compared with some of the catalysts used for this transformation, previously (see Table 3). It is worthy of note that, although the small amounts of catalyst was utilized (4 mol%), it could be separated from the reaction medium simply by using an external magnet and reused for at least six consecutive trials without significant decrease in the catalytic activity.

Most of the obtained triazoles (**4a–j**, **4m–p** and **4r–v**) were known and their physical (color, melting points) and spectral (mass spectrometry) data found to be identical with those of authentic compounds. The selected compounds were further identified by FT-IR, ^{1}H NMR and ^{13}C NMR spectroscopy which compared with literature data. The novel synthesized compounds (**4k**, **4l** and **4q**) were also characterized by using elemental analysis technique.

In the FT-IR spectra of the products, the disappearance of the absorption bands due to C≡C and ≡C–H stretching bands (at about 2250–2100 and 3300 cm^{-1}, respectively) accompanied by the appearance of the characteristic bands due to the out of plane bending vibrations of the =C–H in the triazole ring (at about 815 cm^{-1}), were evidence for the formation of 1,4-disubstituted 1,2,3-triazoles. Also, the FT-IR spectra of all products show absorption bands at about 1293–1217 cm^{-1} (due to N–N=N–) related to the triazole ring. Structural assignments of triazoles were made by comparison of the ^{1}H and ^{13}C NMR spectra with those reported previously. In particular, click condensations were confirmed by the appearance of a singlet resonating at around 8.5–7.5 ppm in ^{1}H NMR spectra, which corresponds to the hydrogen on 5-position of triazole ring and confirms the regioselective synthesis of 1,4-disubstituted triazole regioisomers (see ESI†).

By analogy with our investigation, the plausible mechanistic pathways for the synthesis of 1,4-disubstituted 1,2,3-triazoles with γ-Fe_2O_3@TiO_2-EG-Cu^{II} catalyst are shown in Scheme 3. The one-pot click reaction involves the *in situ* generation of organic azide, in water, within a short reaction time. Copper in the γ-Fe_2O_3@TiO_2-EG-Cu^{II} catalyst promotes the formation of Cu(II)–acetylide complex (**I**) which diminishes the electron density of the alkyne. Subsequently, Huisgen 1,3-dipolar cycloaddition reaction between organic azide and Cu(II)–acetylide complex (**I**) leads to formation of **II**. However, according to the Sharpless *et al.* definition about the "on water" reactions,[37] the significant beneficial effects, in terms of the rates and selectivity of such a reactions have been observed. In this cases, the participated reactants in the reaction are insoluble in aqueous media and therefore the reaction would take place under suspension in water.[38] So, it is worth to note that, the formation of complex (**II**) would be proceed through an "on water" effect, because of the insolubility of organic azides and terminal acetylenes in aqueous media.[38b] Finally, the corresponding 1,2,3-triazole was obtained and the re-generated catalyst re-enters the catalytic cycle. Since the formation of diynes (which usually generated during the reduction process of Cu^{II} to Cu^{I}) was not detected in the present study, we assume that the reaction proceeds *via* a pathway involving Cu^{II} as postulated by

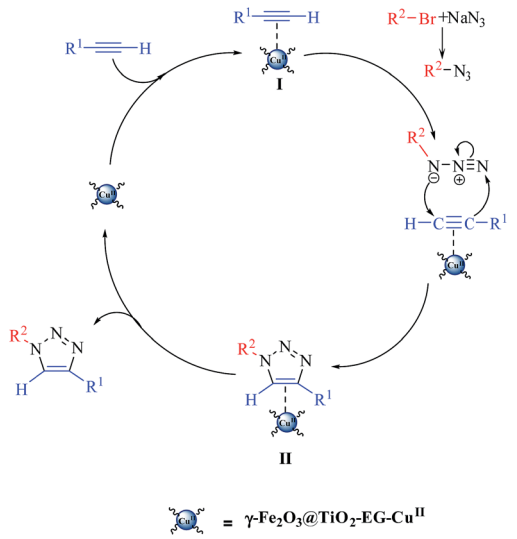

Scheme 3 Plausible reaction mechanism for 1,4-disubstituted 1,2,3-triazole synthesis using γ-Fe_2O_3@TiO_2-EG-Cu^{II}.

Pitchumani *et al.*[26c,e] Further studies to elucidate the details of the mechanism are ongoing.

To investigate the reusability of the catalyst, the reaction of phenylacetylene, benzyl bromide and sodium azide was accomplished under the above-mentioned optimized reaction conditions (Table 1, entry 6). The isolated yield of the product was measured exactly, after the first run. Then, the catalyst was separated by using an external magnet, followed by washing twice with methanol and drying overnight at room temperature. These recovered MNPs were reused in next run under the same reaction conditions. This procedure was repeated six times and in each time the isolated yield of the product was evaluated precisely. As it is shown in Fig. 7 no considerable decrease in the product yield was observed after repeated cycles of the reaction. These results suggest that the catalyst is efficient for six run.

The copper content of freshly prepared γ-Fe_2O_3@TiO_2-EG-Cu^{II} which was obtained by inductively coupled plasma (ICP) was 0.74 mmol of Cu per 1.000 g of γ-Fe_2O_3@TiO_2-EG-Cu^{II}, whilst ICP shows that the 6th reused γ-Fe_2O_3@TiO_2-EG-Cu^{II}

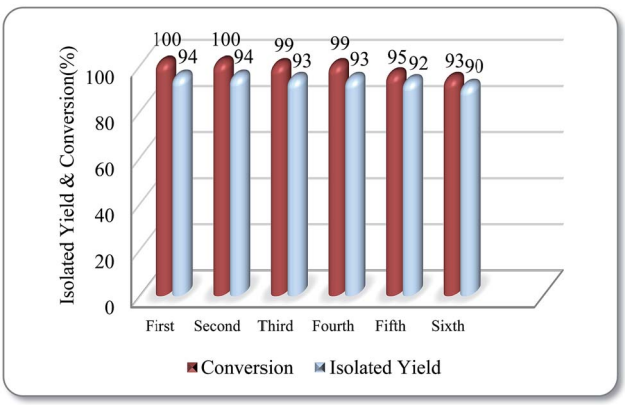

Fig. 7 Synthesis of 1-benzyl-4-phenyl-1*H*-1,2,3-triazole in the presence of the reused γ-Fe_2O_3@TiO_2-EG-Cu^{II}.

contains 0.64 mmol of Cu per 1.000 g of 6th reused γ-Fe_2O_3@TiO_2-EG-Cu^{II}. It means that, the amount of leached metal from the surface of the catalyst is very low.

The FT-IR spectrum of the 6th recovered γ-Fe_2O_3@TiO_2-EG-Cu^{II} was shown in Fig. 1e. As can be seen, the shape, position and relative intensity of all characteristic peaks are well preserved. The results indicate no considerable changes on the chemical structure of functional groups and the hydrogen bonding network.

To show the advantages of γ-Fe_2O_3@TiO_2-EG-Cu^{II} over some of the reported catalysts in the literature, the catalytic performance of γ-Fe_2O_3@TiO_2-EG-Cu^{II} in the synthesis of 1-benzyl-4-phenyl-1*H*-1,2,3-triazole, was compared with various reported catalyst (Table 3). However, some of these methods suffer from one or more of the following drawbacks, such as using environmentally hazardous catalysts or solvents, handling of toxic and hazardous organic azides, using some additives (reducing agents such as sodium ascorbate and hydrazine monohydrate),[14h,44] tedious purification of products and moreover, require long reaction times to achieve reasonable yields. However, such difficulties were removed by using γ-Fe_2O_3@TiO_2-EG-Cu^{II} as an efficient and reusable nanomagnetic catalyst for the synthesis of 1-benzyl-4-phenyl-1*H*-1,2,3-triazole, in water as a green solvent.

4. Conclusion

Conclusively, Cu^{II} immobilized on guanidinated epibromohydrin functionalized γ-Fe_2O_3@TiO_2 (γ-Fe_2O_3@TiO_2-EG-Cu^{II}) as a new heterogeneous catalyst was synthesized and characterized by different techniques such as, FT-IR, TGA/DTA, HRTEM, XRD, EDX, VSM, ICP and CHN. The obtained average particle size of γ-Fe_2O_3 core and TiO_2 shell calculated by HRTEM and XRD was 10–20, 5–10 and 13, 7 nm, respectively. The newly synthesized catalyst showed superior catalytic activity for the synthesis of 1,4-disubstituted 1,2,3-triazoles, through the Huisgen 1,3-dipolar cycloaddition reaction, in the absence of any reducing agent or additive. This one pot preparation of 1,2,3-triazoles involves initial substitution of benzyl/allyl bromides with sodium azide for the *in situ* generation of benzyl/allyl azides, which is followed by γ-Fe_2O_3@TiO_2-EG-Cu^{II} catalyzed cycloaddition reaction without using any reducing agent on water, at 50 °C. Mildness of the reaction conditions, experimental simplicity, compatibility with a wide range of substrates with high functional group tolerance, avoiding the handling of hazardous azides, air atmosphere, using inexpensive reagents, excellent regioselectivity and high yields, short reaction times, easy work-up procedure, using water as a green reaction medium, besides high metal loading capacity and reusability of the catalyst, make this protocol very attractive and environmentally compatible process for the synthesis of a variety of 1,2,3-triazoles.

Acknowledgements

The authors gratefully acknowledge the partial support of this study by Ferdowsi University of Mashhad Research Council (Grant no. p/3/39490).

Notes and references

1 R. Alvarez, S. Velazquez, A. San-Félix, S. Aquaro, E. De Clercq, C. F. Perno, A. Karlsson, J. Balzarini and M. J. Camarasa, *J. Med. Chem.*, 1994, **37**, 4185.
2 S. Velazquez, R. Alvarez, C. Perez, F. Gago, E. De Clercq, J. Balzarini and M. J. Camarasa, *Antiviral Chem. Chemother.*, 1998, **9**, 481.
3 G. Hugo, C. Gilmar, B. Fernando, S. L. Maria Cristina, S. C. Marilia and F. F. Vitor, *J. Braz. Chem. Soc.*, 2007, **18**, 1285.
4 D. R. Buckle, C. J. M. Rockell, H. Smith and B. A. Spicer, *J. Med. Chem.*, 1986, **29**, 2262.
5 L. L. Brockunier, E. R. Parmee, H. O. Ok, M. R. Candelore, M. A. Cascieri, L. F. Colwell, L. Deng, W. P. Feeney, M. J. Forrest, G. J. Hom, D. E. MacIntyre, L. Tota, M. J. Wyvratt, M. H. Fisher and A. E. Weber, *Bioorg. Med. Chem. Lett.*, 2000, **10**, 2111.
6 Q. Dai, W. Gao, D. Liu, L. M. Kapes and X. Zhang, *J. Org. Chem.*, 2006, **71**, 3928.
7 G. C. Tron, T. Pirali, R. A. Billington, P. L Canonico, G. Sorba and A. A. Genazzani, *Med. Res. Rev.*, 2008, **28**, 278.
8 V. Aucagne, K. D. Hänni, D. A. Leigh, P. J. Lusby and D. B. Walker, *J. Am. Chem. Soc.*, 2006, **128**, 2186.
9 W. Q. Fan and A. R. Katritzky, in *Comprehensive Heterocyclic Chemistry II*, ed. A. R. Katritzky, C. W. Ress and E. F. V. Scriven, Elsevier Science, Oxford, 1996, vol. 4, pp. 1–126.
10 (*a*) R. Huisgen, R. Knorr, L. Mobius and G. Szeimies, *Chem. Ber.*, 1965, **98**, 4014; (*b*) R. Huisgen, *Pure Appl. Chem.*, 1989, **61**, 613; (*c*) R. Huisgen, *Angew. Chem., Int. Ed. Engl.*, 1963, **2**, 565; (*d*) L. D. Pachón, J. H. van Maarseveen and G. Rothenberg, *Adv. Synth. Catal.*, 2005, **347**, 811; (*e*) G. Molteni, C. L. Bianchi, G. Marinoni, N. Santo and A. Ponti, *New J. Chem.*, 2006, **30**, 1137; (*f*) A. Sarkar, T. Mukherjee and S. Kapoor, *J. Phys. Chem. C*, 2008, **112**, 3334; (*g*) D. Raut, K. Wankhede, V. Vaidya, S. Bhilare, N. Darwatkar, A. Deorukhkar, G. Trivedi and M. Salunkhe, *Catal. Commun.*, 2009, **10**, 1240; (*h*) P. Cintas, A. Barge, S. Tagliapietra, L. Boffa and G. Cravotto, *Nat. Protoc.*, 2010, **5**, 607; (*i*) E. D. Pressly, R. J. Amir and C. J. Hawker, *J. Polym. Sci., Part A: Polym. Chem.*, 2011, **49**, 814.
11 V. V. Rostovtsev, L. G. Green, V. V. Fokin and K. B. Sharpless, *Angew. Chem., Int. Ed.*, 2002, **41**, 2596.
12 C. W. Tornoe, C. Christensen and M. Meldal, *J. Org. Chem.*, 2002, **67**, 3057.
13 (*a*) V. D. Bock, H. Hiemstra and J. H. van Maarseveen, *Eur. J. Org. Chem.*, 2006, **2006**, 51; (*b*) J. Y. Kim, J. C. Park, H. Kang, H. Song and K. H. Park, *Chem. Commun.*, 2010, **46**, 439.
14 For some selected examples, see: (*a*) C. Shao, X. Wang, J. Xu, J. Zhao, Q. Zhang and Y. Hu, *J. Org. Chem.*, 2010, **75**, 7002; (*b*) C. Deraedt, N. Pinaud and D. Astruc, *J. Am. Chem. Soc.*, 2014, **136**, 12092; (*c*) K. B. Mishra and V. K. Tiwari, *J. Org. Chem.*, 2014, **79**, 5752; (*d*) H. K. Akula and M. K. Lakshman, *J. Org. Chem.*, 2012, **77**, 8896; (*e*) J. T. Fletcher and J. E. Reilly, *Tetrahedron Lett.*, 2011, **52**, 5512; (*f*) S. Dörner and B. Westermann, *Chem. Commun.*, 2005, 2852; (*g*) Y. Jiang, D. Kong, J. Zhao, Q. Qi, W. Li and G. Xu, *RSC Adv.*, 2014, **4**,

1010; (*h*) A. Pathigoolla, R. P. Pola and K. M. Sureshan, *Appl. Catal., A*, 2013, **453**, 151.

15 (*a*) S. Quader, S. E. Boyd, I. D. Jenkins and T. A. Houston, *J. Org. Chem.*, 2007, **72**, 1962; (*b*) P. Appukkuttan, W. Dehaen, V. V. Fokin and E. Van der Eycken, *Org. Lett.*, 2004, **6**, 4223.

16 For some selected examples, see: (*a*) A. Marra, A. Vecchi, C. Chiappe, B. Melai and A. Dondoni, *J. Org. Chem.*, 2008, **73**, 2458; (*b*) S. Ozçubukçu, E. Ozkal, C. Jimeno and M. A. Pericàs, *Org. Lett.*, 2009, **11**, 4680; (*c*) I. Cano, M. C. Nicasio and P. J. Pérez, *Org. Biomol. Chem.*, 2010, **8**, 536; (*d*) J. García-Álvarez, J. Díez and J. Gimeno, *Green Chem.*, 2010, **12**, 2127; (*e*) T. R. Chan, R. Hilgraf, K. B. Sharpless and V. V. Fokin, *Org. Lett.*, 2004, **6**, 2853; (*f*) W. G. Lewis, F. G. Magallon, V. V. Fokin and M. G. Finn, *J. Am. Chem. Soc.*, 2004, **126**, 9152; (*g*) V. O. Rodionov, S. I. Presolski, S. Gardinier, Y. H. Lim and M. G. Finn, *J. Am. Chem. Soc.*, 2007, **129**, 12696; (*h*) V. O. Rodionov, S. I. Presolski, D. Diaz Diaz, V. V. Fokin and M. G. Finn, *J. Am. Chem. Soc.*, 2007, **129**, 12705; (*i*) S. Díez-González and S. P. Nolan, *Angew. Chem., Int. Ed.*, 2008, **47**, 8881; (*j*) S. Díez-González, *Catal. Sci. Technol.*, 2011, **1**, 166; (*k*) S. Guo, M. H. Lim and H. V. Huynh, *Organometallics*, 2013, **32**, 7225; (*l*) H. D. Velázquez, Y. R. García, M. Vandichel, A. Madder and F. Verpoort, *Org. Biomol. Chem.*, 2014, **12**, 9350.

17 (*a*) A. Coelho, P. Diz, O. Caamaño and E. Sotelo, *Adv. Synth. Catal.*, 2010, **352**, 1179; (*b*) C. Girard, E. Önen, M. Aufort, S. Beauvie`re, E. Samson and J. Herscovici, *Org. Lett.*, 2006, **8**, 1689.

18 I. S. Park, M. S. Kwon, Y. Kim, J. S. Lee and J. Park, *Org. Lett.*, 2008, **10**, 497.

19 (*a*) B. H. Lipshutz and B. R. Taft, *Angew. Chem.*, 2006, **118**, 8415; (*b*) B. H. Lipshutz and B. R. Taft, *Angew. Chem., Int. Ed.*, 2006, **45**, 8235.

20 (*a*) S. Chassaing, A. S. S. Sido, A. Alix, M. Kumarraja, P. Pale and J. Sommer, *Chem.–Eur. J.*, 2008, **14**, 6713; (*b*) S. Chassaing, M. Kumarraja, A. S. S. Sido, P. Pale and J. Sommer, *Org. Lett.*, 2007, **9**, 883.

21 A. Megia-Fernandez, M. Ortega-Muñoz, J. Lopez-Jaramillo, F. Hernandez-Mateo and F. Santoyo-Gonzalez, *Adv. Synth. Catal.*, 2010, **352**, 3306.

22 (*a*) M. L. Kantam, V. S. Jaya, B. Sreedhar, M. M. Rao and B. M. Choudary, *J. Mol. Catal. A: Chem.*, 2006, **256**, 273; (*b*) T. Katayama, K. Kamata, K. Yamaguchi and N. Mizuno, *ChemSusChem*, 2009, **2**, 59.

23 I. Jlalia, H. Elamari, F. Meganem, J. Herscovici and C. Girard, *Tetrahedron Lett.*, 2008, **49**, 6756.

24 T. Miao and L. Wang, *Synthesis*, 2008, **3**, 363.

25 K. Yamaguchi, T. Oishi, T. Katayama and N. Mizuno, *Chem.–Eur. J.*, 2009, **15**, 10464.

26 (*a*) A. N. Prasad, B. M. Reddy, E. Y. Jeong and S. E. Park, *RSC Adv.*, 2014, **4**, 29772; (*b*) M. Tajbakhsh, M. Farhang, S. M. Baghbanian, R. Hosseinzadeh and M. Tajbakhsh, *New J. Chem.*, 2015, **39**, 1827; (*c*) K. Namitharan, M. Kumarraja and K. Pitchumani, *Chem.–Eur. J.*, 2009, **15**, 2755; (*d*) B. S. P. Anil Kumar, K. Harsha Vardhan Reddy, K. Karnakar, G. Satish and Y. V. D. Nageswar, *Tetrahedron Lett.*, 2015, **56**, 1968; (*e*) N. Mukherjee, S. Ahammed, S. Bhadra and B. C. Ranu, *Green Chem.*, 2013, **15**, 389; (*f*) Y. Masuyama, K. Yoshikawa, N. Suzuki, K. Hara and A. Fukuoka, *Tetrahedron Lett.*, 2011, **52**, 6916.

27 (*a*) D. Lee, J. Lee, H. Lee, S. Jin, T. Hyeon and B. M. Kim, *Adv. Synth. Catal.*, 2006, **348**, 41; (*b*) C. O. Dalaigh, S. A. Corr, Y. Gunko and S. J. Connon, *Angew. Chem., Int. Ed.*, 2007, **46**, 4329; (*c*) Y. Zheng, P. D. Stevens and Y. Gao, *J. Org. Chem.*, 2006, **71**, 537; (*d*) S. Ding, Y. Xing, M. Radosz and Y. Shen, *Macromolecules*, 2006, **39**, 6399.

28 S. Sobhani and R. Jahanshahi, *New J. Chem.*, 2013, **37**, 1009.

29 (*a*) L. Levy, Y. Sahoo, K. S. Kim, E. J. Bergey and P. N. Prasad, *Chem. Mater.*, 2002, **14**, 3715; (*b*) S. Sacanna, L. Rossi and A. P. Phillipse, *Langmuir*, 2007, **23**, 9974; (*c*) A. Xia, J. Hu, C. Wang and D. Jiang, *Small*, 2007, **3**, 1811.

30 F. Nador, M. A. Volpe, F. Alonso, A. Feldhoff, A. Kirschning and G. Radivoy, *Appl. Catal., A*, 2013, **455**, 39.

31 (*a*) N. Razavi and B. Akhlaghinia, *RSC Adv.*, 2015, **5**, 12372; (*b*) S. S. E. Ghodsinia and B. Akhlaghinia, *RSC Adv.*, 2015, **5**, 49849; (*c*) M. Zarghani and B. Akhlaghinia, *Appl. Organomet. Chem.*, 2015, **29**, 683; (*d*) Z. Zarei and B. Akhlaghinia, *Chem. Pap.*, 2015, **69**, 1421; (*e*) M. Zarghani and B. Akhlaghinia, *RSC Adv.*, 2015, **5**, 87769; (*f*) N. Razavi and B. Akhlaghinia, *New J. Chem.*, 2016, **40**, 477; (*g*) R. Jahanshahi and B. Akhlaghinia, *RSC Adv.*, 2015, **5**, 104087; (*h*) N. Yousefi Siavashi, B. Akhlaghinia and M. Zarghani, *Res. Chem. Intermed.*, 2016, DOI: 10.1007/s11164-015-2404-8; (*i*) E. Karimian, B. Akhlaghinia and S. S. E. Ghodsinia, *J. Chem. Sci.*, 2016, **128**, 429.

32 L. Yu, X. Peng, F. Ni, J. Li, D. Wang and Z. Luan, *J. Hazard. Mater.*, 2013, **246–247**, 10.

33 S. Sobhani, Z. Vahidi, Z. Zeraatkar and S. Khodadadi, *RSC Adv.*, 2015, **5**, 36552.

34 A. Banisharif, S. Hakim Elahi, A. Anaraki Firooz, A. A. Khodadadi and Y. Mortazavi, *International Journal of NanoScience and Nanotechnology*, 2013, **9**, 193.

35 (*a*) Y. Gao, Y. Masuda, Z. Peng, T. Yonezawa and K. Koumoto, *J. Mater. Chem.*, 2003, **13**, 608; (*b*) B. Klingenberg and M. A. Vannice, *Chem. Mater.*, 1996, **8**, 2755; (*c*) A. Rostami, B. Atashkar and D. Moradi, *Appl. Catal., A*, 2013, **467**, 7.

36 F. Adam, K. M. Hello and H. Osman, *Chin. J. Chem.*, 2010, **28**, 2383.

37 S. J. Narayan, M. G. Muldoon, V. V. Finn, H. C. Fokin and K. B. K. Sharpless, *Angew. Chem., Int. Ed.*, 2005, **44**, 3275.

38 (*a*) E. Soleimani, S. Ghorbani, M. Taran and A. Sarvary, *C. R. Chim.*, 2012, **15**, 955; (*b*) H. X. Siyang, H. L. Liu, X. Y. Wu and P. N. Liu, *RSC Adv.*, 2015, **5**, 4693.

39 K. R. Reddy, K. Rajgopal and M. L. Kantam, *Synlett*, 2006, **6**, 957.

40 L. Huang, W. Liu, J. Wu, Y. Fu, K. Wang, C. Huo and Z. Du, *Tetrahedron Lett.*, 2014, **55**, 2312.

41 W. Wang, J. Wu, C. Xia and F. Li, *Green Chem.*, 2011, **13**, 3440.

42 H. Sharghi, R. Khalifeh and M. M. Doroodmand, *Adv. Synth. Catal.*, 2009, **351**, 207.

43 M. Gupta, M. Gupta, S. Paul, R. Kant and V. K. Gupta, *Monatsh. Chem.*, 2015, **146**, 143.

44 F. Matloubi Moghaddam and S. E. Ayati, *RSC Adv.*, 2015, **5**, 3894.